DISCLAIMER NOTICE

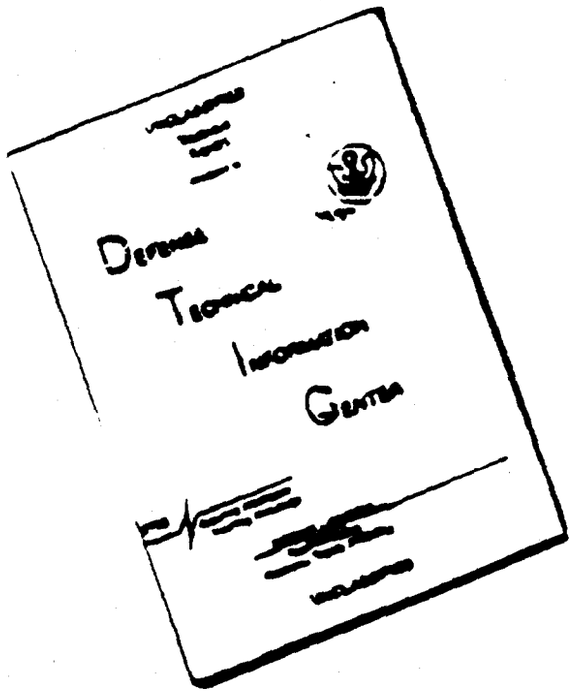

THIS DOCUMENT IS BEST QUALITY AVAILABLE. THE COPY FURNISHED TO DTIC CONTAINED A SIGNIFICANT NUMBER OF PAGES WHICH DO NOT REPRODUCE LEGIBLY.

This information is inaccurate, correct title appears on p 1.

SEMI-ANNUAL REPORT

AN INVESTIGATION OF ADHESIVE/ADHEREND AND FIBER MATRIX INTERACTIONS

by

Betty Beck, Ranjani Siriwardane and James P. Wightman

Prepared for

National Aeronautics and Space Administration

September, 1981

Grant NAG-1-127

NASA-Langley Research Center
Hampton, Virginia 23665
Materials Division
Donald J. Progar

Department of Chemistry
Virginia Polytechnic Institute and State University
Blacksburg, Virginia 24061

SUMMARY

Research during the report period March 1 to August 31, 1981 has focused on the following areas:

- Continued SEM/ESCA analysis of lap shear samples received from the Boeing Company under NASA Contract NAS1-15605.
- SEM/ESCA analysis of flatwise tensile specimens.
- Surface characterization of TiO_2, Ti 6-4 and Ti powders with particular emphasis on their interaction with primer solutions of both polyphenylquinoxaline and LaRC-13 polyimide.

Details of the above areas will be contained in the Final Technical Report. A preprint of a paper scheduled to appear in the next issue of SAMPE Quarterly is appended. This paper summarizes some of the work done in the first area listed above.

See PL-437748

SAMPE Quarterly, Vol 13, no 1 Oct 81

The Application of Surface Analysis to Polymer/Metal Adhesion

James P. Wightman
Chemistry Department
Virginia Polytechnic Institute and State University
Blacksburg, VA 24061

The use of scanning electron microscopy (SEM) and x-ray photoelectron spectroscopy (XPS) in the analysis of ~~Ti 6-4~~ adherend surfaces is described. Differences in Ti 6-4 surface composition as determined by XPS after different chemical pretreatments are detailed. Analysis of fractured surfaces by SEM/XPS is used to establish the failure mode. The surface acidity of Ti 6-4 coupons can be established by reflectance visible spectroscopy using indicator dyes.

Introduction

A long-term, continuing NASA goal (1) is to develop improved adhesives and composite matrices for high temperature supersonic transport technology. The extreme conditions encountered in application of this technology demand a unique combination of processability, toughness and durability. One aspect of this multi-faceted program is the development of an autoclaveable, high-temperature adhesive system for joining titanium/titanium, titanium/composite, and composite/composite intended to serve structurally for thousands of hours at 505 K (450°F). One part of the total effort properly involves surface analysis. Our primary emphasis (2) has been on the microscopic/spectroscopic characterization of Ti 6-4 adherend surfaces prior to adhesive bonding and following fracture, is discussed The experimental techniques used ~~in our~~ studies are outlined ~~in Table I.~~ of (author, modified - PL)

Adherend Surface Morphology/Composition

Scanning electron microscopy (SEM) and x-ray photoelectron spectroscopy (XPS) couple to give a unique "fingerprint" for each particular chemical pretreatment of Ti 6-4 adherends. This conclusion is based on the results shown in Fig. 1 and Table II. SEM is a well known technique (3) and is widely used in adhesion studies (4). Representative SEM photomicrographs (5) of Ti 6-4 after four different pretreatments are shown in Fig. 1. For the chromic acid anodized (CAA) surface seen in Fig. 1A, there appears to be a surface layer containing minute cracks or fissures of irregular shape. At the highest magnification (X 10,000), the whole surface layer appears to be sponge-like presumably due to the presence of small diameter pores not resolved in the SEM. The surface features for the phosphoric acid anodized (PAA) Ti 6-4 surface shown in Fig. 1B are similar to those described for the CAA case.

The surface morphology for the Turco (TU) etched surface seen in Fig. 1C is in sharp contrast to that following the anodizing pretreatments. The beta phase appears to have grown at the expense of the alpha phase and exists as highly fragmented structures. The alkaline hydrogen peroxide BAE process produces the surface seen in Fig. 1D where the surface features are unlike any of the preceding ones. A mottled surface is obtained containing no distinct features.

The XPS technique (6) involves the measurement of the energy and intensity of photoelectrons ejected from a solid sample under x-ray bombardment. The identification of elements and the assignment of the chemical state of those elements in the top 5 nm of a solid surface is possible with XPS. Representative XPS results for Ti 6-4 adherends (5) are shown in Table II for the same four pretreatments noted in Fig. 1. The binding energies (B.E.) in eV for each observed photopeak are tabulated along with calculated values

of the atomic fractions (A.F.). The F 1s photopeak assigned to the fluoride ion, appears on both anodized surfaces but not on the TU or RAE treated surface. Two F 1s photopeaks are noted on the CAA surfaces suggesting that F is present in two different bonding states on that surface. The O 1s photopeak arising from the surface oxide layer is constant at 529.6 $\pm$ 0.2 eV across all four surfaces. Similarly, the Ti 2p3 photopeak, assigned to the tetravalent state of titanium and present as titanium dioxide (TiO_2), is constant at 458.0 $\pm$ 0.1 eV. The assignment of the N 1s photopeak at a constant value of 399.4 $\pm$ 0.1 eV is uncertain though it could be due to nitride formation with titanium. Calcium and phosphorus are detected as residuals after the RAE and PAA processes, resp.

The effect of thermal aging on the morphology of a freshly pretreated Ti 6-4 surface is illustrated dramatically in the SEM photomicrographs in Fig. 2. Here, a TU pretreated Ti 6-4 coupon was placed in a forced air oven at 498 K (450°F) for 10 hours. The SEM photomicrographs of the unheated sample are shown in Fig. 2A. A comparison of Fig. 2B with Fig. 2A demonstrates the marked change in surface morphology accompanying thermal aging. The implication of this gross change of physical structure in bond durability studies at elevated temperatures is clear.

Failure mode analysis

SEM/XPS analysis of fractured surfaces can be used to establish the failure mode. The SEM photomicrographs in Fig. 3 suggest a shift from a mixed (interfacial/cohesive) failure mode seen in Fig. 3B to pure cohesive failure seen in Fig. 3A on addition of a siloxane elastomer to a LaRC-13 polyimide adhesive. The synthesis of LaRC-13 polyimide adhesives has been described (7,8). The XPS results in Table III complement the above SEM results in that one member of the fractured lap shear specimen bonded <u>without</u> the elastomer

gives a significant Ti photopeak. The fact that this photopeak is observed suggests appreciable interfacial failure. This is a significant conclusion since using XPS, the old argument of cohesive versus adhesive failure can now be documented down to the 2 nm level. No Ti photopeak is observed for either member of the fractured lap shear specimen bonded with the elastomer indicative of cohesive failure. Supporting evidence for the failure mode assignments is obtained from other XPS photopeaks. For example, when LaRC-13 adhesive remains on the Ti 6-4 adherend, the binding energy of the O 1s photopeak shifts by 1.5 eV from 530.1 to 531.6 eV. The lower binding energy photopeak is characteristic of oxygen in the titanium dioxide surface layer (see Table II). Note that the smaller Si 2p and F 1s photopeaks observed for the 'no elastomer' case are due to scrim cloth and pretreatment residuals, resp. On the other hand, the larger Si 2p and F 1s photopeaks observed for the 'elastomer' case are due to the fluorosiloxane additive.

Similar XPS results are shown in Table IV for the analysis of a fractured T-peel specimen of Ti 6-4 bonded in this case with an epoxy. The unbonded (#1) adherend and one of the fracture members (#3) give very similar results. This suggests fracture within the surface oxide layer rather than at the oxide/epoxy interface. In the latter instance, XPS results characteristic of the epoxy would have been observed which was not the case. Further, the unbonded (#1) adherend and the same fracture member (#3) show only a tetravalent titanium [Ti(IV)] photopeak again characteristic of a titanium dioxide surface layer. It is instructive indeed that the other fracture member (#2) gives an elemental Ti(0) photopeak at a binding energy 3.5 eV lower than Ti (IV). The Ti(0) photopeak would only be observed if failure occurred not just within the oxide layer but also close to the base adherend. This conclusion is summarized schematically in the idealized diagram

in Fig. 4.

SEM photomicrographs of a fractured lap shear sample bonded with polyphenylquinoxaline (PPQ) are shown in Fig. 5. The synthesis of PPQ has been described elsewhere (9,10). The PPQ bonded CAA Ti 6-4 adherends gave a measured lap shear strength at room temperature of 4650 psi. It is clear that no features characteristic of the Ti 6-4 adherend are seen in the photomicrographs; thus, the sample failed cohesively. The XPS results for the fraction surface are shown in Table V. No Ti photopeak was observed, confirming cohesive failure. The O 1s, N 1s and C 1s photopeaks are characteristic of PPQ. Note the shift in the binding energy of the O 1s photopeak compared to the adherend (see Table II). The Si 2p photopeak is due to the glass scrim cloth which is seen in the SEM photomicrographs.

By contrast, a lap shear strength of 1950 psi was determined in the case of phosphate-fluoride (P-F) treated Ti 6-4 adherends bonded with PPQ. Apparent interfacial feature is noted from the SEM photomicrographs of the fracture surfaces in Fig. 6A and 6B. The metal failure surface (MFS) in Fig. 6A shows a surface morphology characteristic of P-F etched Ti 6-4 surfaces. The adhesive failure surface (AFS) in Fig. 6B shows the "imprint" of the adherend. Closer inspection shows micro-voids in the adhesive left after pull-out of the β phase.

The P-F surface pretreatment invariably led to debonding of the adhesive slab when punched for XPS sample preparation. The various fracture surfaces are depicted schematically in Fig. 7. The SEM photomicrograph of the metal substrate surface (MSS) and the adhesive substrate surface (ASS) are shown in Figs. 6C and 6D. Similar features are noted in these photomicrographs as were seen in Figs. 6A and 6B.

The XPS results for the four surfaces are shown in Table VI. The AFS (Fig. 6A) shows a significant Ti signal which fact is further confirmation of the assignment of interfacial failure for this sample. The photopeak at a binding energy of 529.5 eV is assigned to oxygen in the surface oxide layer. We have reported (11) a value of 529.5 eV for the O 1s photopeak following P-F treatment of Ti 6-4. Thus, the ESCA results support the existence of a titanium oxide layer on the metal failure surface. Ca is present as a residual on the Ti 6-4 adherend surface after the P-F treatment. The N 1s photopeak at 398.3 eV is consistent with the N 1s photopeak observed for the Ti 6-4 adherend surface after any chemical pretreatment (see Table II). However, the origin of the nitrogen is not clear since a N 1s photopeak at about the same binding energy is observed for both pretreated Ti 6-4 and for PPQ (see Table V). The observation of a significant Si 2s photopeak is quite interesting. Again, the origin of this Si signal is not clear. However, the fact that failure occurred at this interface may be associated with the presence of silicon. The SEM photomicrographs (see Fig. 6A) shows no evidence of glass fragment from the scrim cloth. It is known that the scrim cloth is coated with an organo-silicon compound. Does in fact degradation and subsequent migration of silicon-containing compounds to the interface occur? The answer to this question will involve additional experiments.

The AFS gives an O 1s photopeak at 531.7 eV (see Table VI) characteristic of PPQ (see Table V). Again, a significant Si signal is observed on this surface where no glass fibers are seen (see Fig. 6C). The absence of a Ti photopeak is additional confirmation of interfacial failure. A further conclusion can be drawn. Failure occurred at the primer/oxide interface rather than in the oxide layer in which case a Ti signal should have been observed.

The MSS (Fig. 6C) shows an O 1s photopeak at 529.2 eV characteristic of the pretreated Ti 6-4. In this case a small V peak and a significant Ti peak were detected. The presence of Ca is consistent with the composition of a P-F treated Ti 6-4 surface. The presence of a trace quantity of lead on this surface and on the adhesive substrate is not explained. The ASS (Fig. 6D) shows an O 1s photopeak at 532.2 eV characteristic of PPQ. A small Ti peak was detected here indicative of fracture of the oxide layer. No silicon was noted on either of these substrate surfaces.

Reflectance spectroscopy both in the infrared (12) and visible regions has been used in the analysis of fractured samples and in the determination of adherend surface acidity. No sample preparation is necessary in the specular reflectance infrared (ir) analysis of fractured samples; the sample is simply inserted into the reflectance sample holder. A typical ir reflectance spectrum (13) of a fractured thermoplastic polyimide (14) bonded Ti 6-4 lap shear sample is shown in Fig. 8. The reflectance spectrum is similar to the more common transmission spectrum. Indeed, the observed peaks correspond to vibrations characteristic of the polyimide. Thus, a relatively thick polyimide film remains on the Ti 6-4 coupon following fracture.

Adherend Surface Acidity

Diffuse reflectance visible spectroscopy (11) has been used to monitor changes in the absorption spectra of acid-base indicators deposited from aqueous solution on Ti 6-4 adherends after various pretreatments. The results of the surface acidity measurements are listed in Table VII. Note that bromthymol blue does not change color on a TU treated Ti 6-4 surface but does change color given a P-F pretreatment. Thus, the TU and P-F treated Ti 6-4 surfaces are basic (pK_a : 7.3-9.2) and acidic (pK_a : 4.9-7.3), resp. Further, as inferred from the results in Table VIII, the phosphate-fluoride

treated Ti 6-4 surfaces decreases in acidity with time. A new peak appears at 630 nm in the reflectance spectrum after 10 hours exposure to the laboratory environment. This conclusion is a surface chemistry basis for the practice of priming freshly pretreated adherend surfaces for "protection" prior to bonding.

Summary

Basic questions in adhesion science for example, failure mode, surface acidity and bond durability can be approached with increasing confidence given the availability of surface analytical techniques including those listed in Table I.

Acknowledgements

This work has been supported by NASA-LaRC under Grant Nos. NSG-1124 and NAG-1-127. Personnel contributing to this research at Virginia Polytechnic Institute and State University were T. A. Bush, Dr. M. E. Counts, Dr. D. W. Dwight, W. Chen, R. Siriwardane and B. Beck.

References

(1) P. M. Hergenrother and N. J. Johnston in ACS Symposium Series No. 132, Resins for Aerospace, C. A. May, Ed., pp 3-13, Am. Chem. Soc., Washington (1980).

(2) B. Beck, R. Siriwardane and J. P. Wightman, NASA Final Report, Grant NSG-1124, NASA-Langley Research Center, VA (1981).

(3) O. Johari and A. V. Samudra in Characterization of Solid Surfaces, P. F. Kane and G. B. Larrabee, Eds., pp. 107-131, Plenum, New York (1974).

(4) D. W. Dwight, M. E. Counts and J. P. Wightman in Colloid and Interface Science, Vol. III, M. Kerker, Ed., pp 143-156, Academic Press, New York (1976).

(5) W. Chen, R. Siriwardane and J. P. Wightman in Proc. 12th SAMPE Techn. Conf., M. Smith, Ed., pp 896-903, SAMPE, Azusa, CA (1980).

(6) K. Siegbahn et al., ESCA-Atomic, Molecular and Solid State Structure Studied by Means of Electron Spectroscopy, Almquist and Wiksells, Upsalla (1967).

(7) A. K. St. Clair and T. L. St. Clair, Polym. Eng. Sci., 16(5), 314 (1976).

(8) T. L. St. Clair and D. J. Progar, Proc. 24th Natl. SAMPE Symp., 24(2), 1081 (1979).

(9) P. M. Hergenrother, J. Macromolecular Sci. - Reviews in Macromol. Chem. C19(1), 1 (1980).

(10) P. M. Hergenrother, Polym. Eng. Sci., in press.

(11) J. G. Mason, R. Siriwardane and J. P. Wightman, J. Adhesion, 11, 315 (1981).

(12) N. J. Harrick, Internal Reflection Spectroscopy, Interscience, New York (1967).

(13) T. A. Bush, M. E. Counts and J. P. Wightman, in Adhesion Science and Technology, Part A, L.-H. Lee, Ed., pp. 365-394, Plenum Press, New York (1975).

(14) D. J. Progar, V. L. Bell and T. L. St. Clair, U. S. Patent 4,065, 345, NASA-LaRC, December, 1977.

TABLE I

EXPERIMENTAL TECHNIQUES USED IN SURFACE ANALYSIS

CHARACTERIZATION OF ADHEREND SURFACES

Surface Morphology - Scanning Electron Microscopy [SEM]

Surface Composition - X-ray Photoelectron Spectroscopy [XPS]

Surface Acidity - Diffuse Reflectance Visible Spectroscopy

CHARACTERIZATION OF FRACTURE SURFACES

Surface Morphology - Scanning Electron Microscopy

Surface Composition - X-ray Photoelectron Spectroscopy

- Specular Reflectance Infrared Spectroscopy

TABLE II

XPS ANALYSIS OF Ti 6-4 SURFACES AFTER CHEMICAL PRETREATMENT

Photopeak	Chromic acid anodize		Phosphoric acid anodize		Turco		RAE	
	B.E.(eV)	A.F.	B.E.(eV)	A.F.	B.E. (eV)	A.F.	B.E.(eV)	A.F
F 1s	687.6			---		---		---
	684.4	0.03	684.4	0.02		---		---
O 1s	529.4	0.19	529.6	0.24	530.0	0.30	529.4	0.4
Ti 2p3	457.8	0.08	458.2	0.10	458.0	0.09	458.0	0.1
N 1s	399.2	0.03	399.4	0.01	399.5	0.01	399.4	0.0
Ca 2p3		---		---		---	346.4	0.0
C 1s	(284.0)	0.67	(284.0)	0.60	(284.0)	0.60	(284.0)	0.2
P 2p3		---	133.0	0.02		---		---
Al 2s		---		---		---	118.2	0.0

TABLE III

XPS ANALYSIS OF FRACTURED T-PEEL Ti 6-4 SAMPLES

Photopeak	LaRC with no elastomer				LaRC-13 with elastomer			
	A side		B side		A side		B side	
	B.E.(eV)	A.F.	B.E.(eV)	A.F.	B.E.(eV)	A.F.	B.E.(eV)	A.F.
F 1s	686.9	0.01	686.9	<0.01	686.8	0.03	686.7	0.07
O 1s	531.4	0.10	530.1	0.19	531.8	0.17	531.6	0.17
Ti 2p3		—	457.3	0.04		—		—
N 1s	399.0	0.03	399.1	0.03	398.8	0.01	398.2	<0.01
C 1s	(284.0)	0.85	(284.0)	0.69	(284.0)	0.58	(284.0)	0.58
Ni 2p	101.4	0.01	100.9	0.05	101.8	0.17	101.7	0.17

TABLE IV

ATOMIC FRACTIONS OF ANODIZED Ti 6-4 SAMPLES BEFORE (#1) AND AFTER FRACTURE (#2, #3)

Photopeak	Atomic Fraction		
	#1	#2	#3
F 1s	0.012	0.004	0.024
O 1s	0.13	0.24	0.17
V 2p3	0.001	0.001	NSP
Ti(IV) 2p3	0.069	0.078	0.071
Ti(O) 2p3	NSP*	0.004	NSP
N 1s	0.006	0.007	0.009
C 1s	0.77	0.66	0.71
Cl 2p	0.004	0.003	NSP
Al 2s	0.01	0.013	0.014

*NSP - no significant peak

TABLE V

XPS ANALYSIS OF FRACTURED PPQ/CAA Ti 6-4 LAP SHEAR SAMPLE

Photopeak	B.E. (eV)	A.F.
O 1s	534.0	0.15
Ti 2p3		--
N 1s	399.1	0.04
C 1s	288.5	0.65
	(284.0)	
Si 2p	102.6	0.16

TABLE VI

XPS ANALYSIS OF FRACTURE SURFACES OF ADHESIVELY BONDED T1 6-4

Photopeak	MFS		AFS		MSS*		ASS*	
	B.E.(eV)	A.F.#	B.E.(eV)	A.F.#	B.E.(eV)	A.F.#	B.E.(eV)	A.F.#
O 1s	531.3	0.27	531.7	0.13		--	532.2	0.07
	529.5				529.2	0.27		
V 2p3		--		--	514.1	<0.01		--
Ti 2p3	457.9	0.04		--	457.9	0.07	458.6	<0.01
N 1s	398.3	0.02	398.3	0.05	398.4	0.02	398.0	0.06
Ca 2p3	346.5	0.01		--	346.5	0.01		--
Si 2s	152.5	0.05	152.6	0.03		--		--

Trace Pb noted in both of these samples.

#Balance is due to carbon.

TABLE VII

λ_{max} VALUES AND COLOR CHANGES OF

INDICATORS ON PRETREATED Ti 6-4 SURFACES

		Turco		Phosphate-Fluoride	
Indicator	pKa at zero ionic strength	Color change before drying	Color and λ_{max} (nm) value after drying	Color change before drying	Color and λ_{max}(nm) value after drying
Benzeneazo-diphenyl-amine	1.5	Y→Y	464 Y	Y→Y	436 Y
Bromphenol blue	4.1	B→B	635 B	B→B	636 B
Bromcresol green	4.9	G→B-G	644 B-G	G→B-G	610 B-G
Bromthymol blue	7.3	B→B	604 B	B→Y-B	464 Y
Thymol blue	9.2	B→Y	476 Y	B→Y	478 Y

B = Blue G = Green Y = Yellow

B-G = Blue-Green Y-B = Yellow Blue

TABLE VIII

TIME EFFECT ON THE ACIDITY OF PHOSPHATE-FLUORIDE ETCHED Ti 6-4 SURFACES USING BROMTHYMOL BLUE

Time (hours)	Color changes before drying	Color changes and λ_{max} (nm) values after drying
1	B → B-Y	444 (Y)
2	B → B-Y	440 (Y)
5	B → B-Y	448 (Y)
10	B → B-Y	400(Y); 630(B)
25	B → B-Y	456(Y); 652(B)
50	B → B-Y	424(Y); 648(B)
100	B → B-Y	444(Y); 632(B)

B-Blue Y-Yellow

1

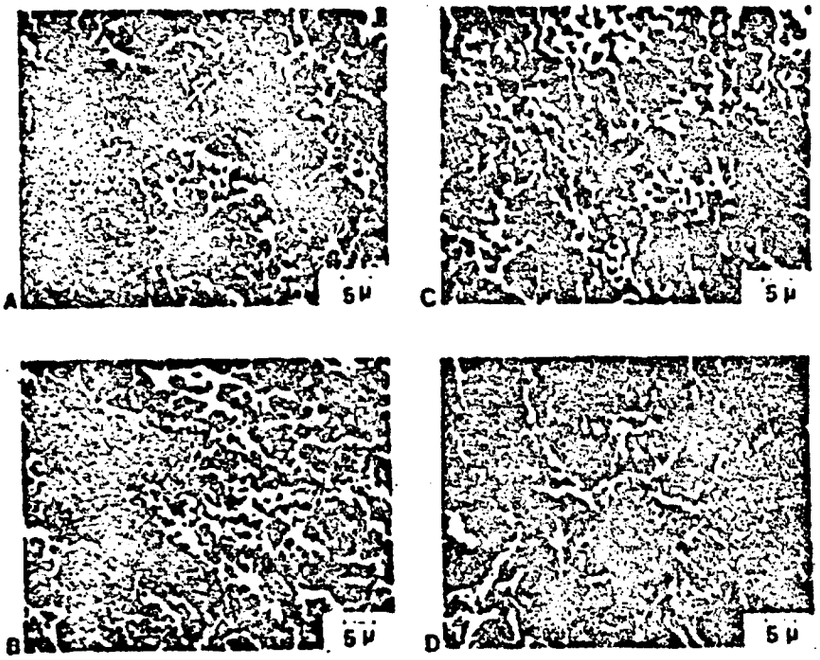

2

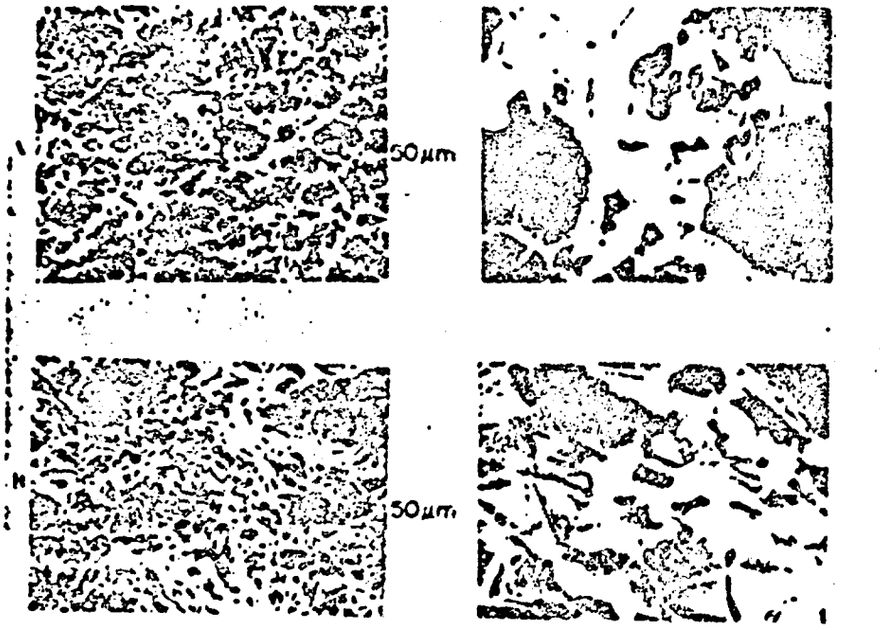

3A

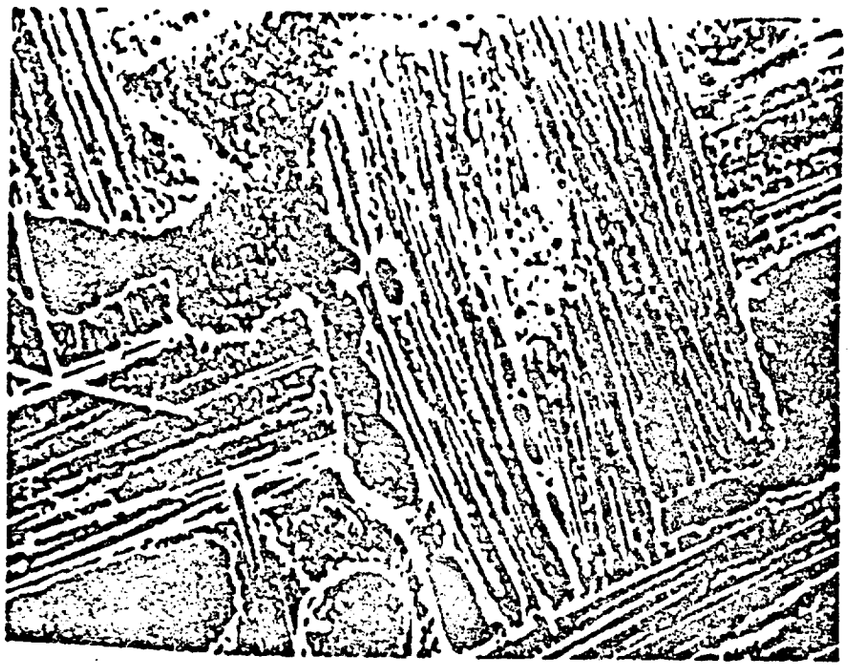

3B

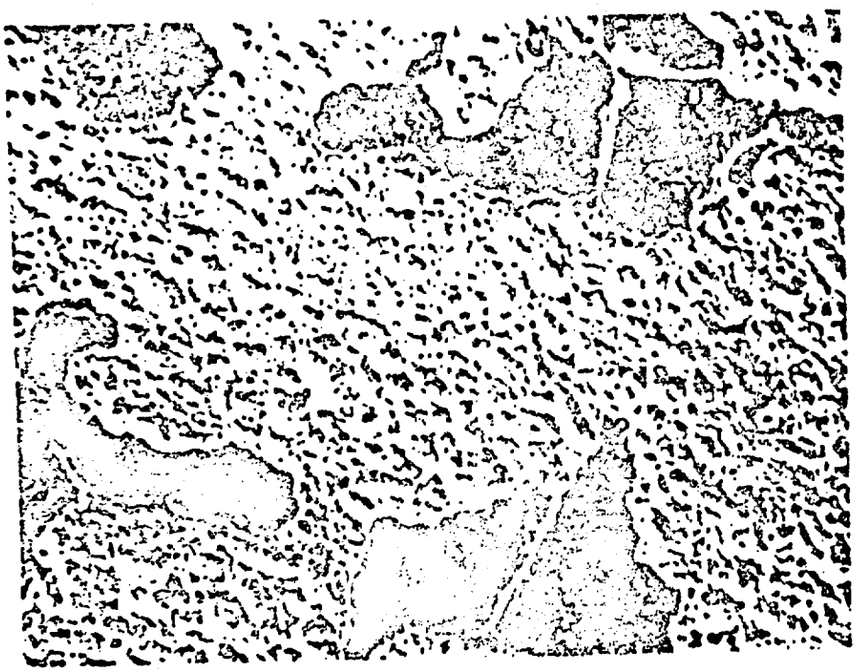

4

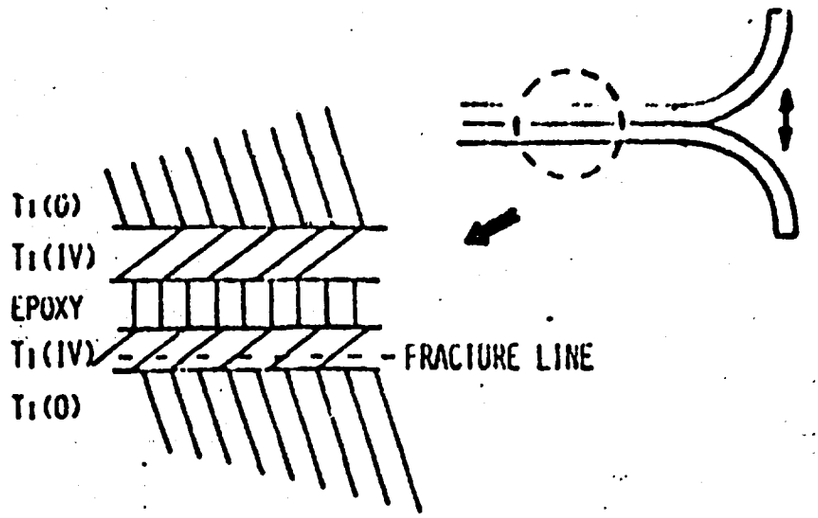

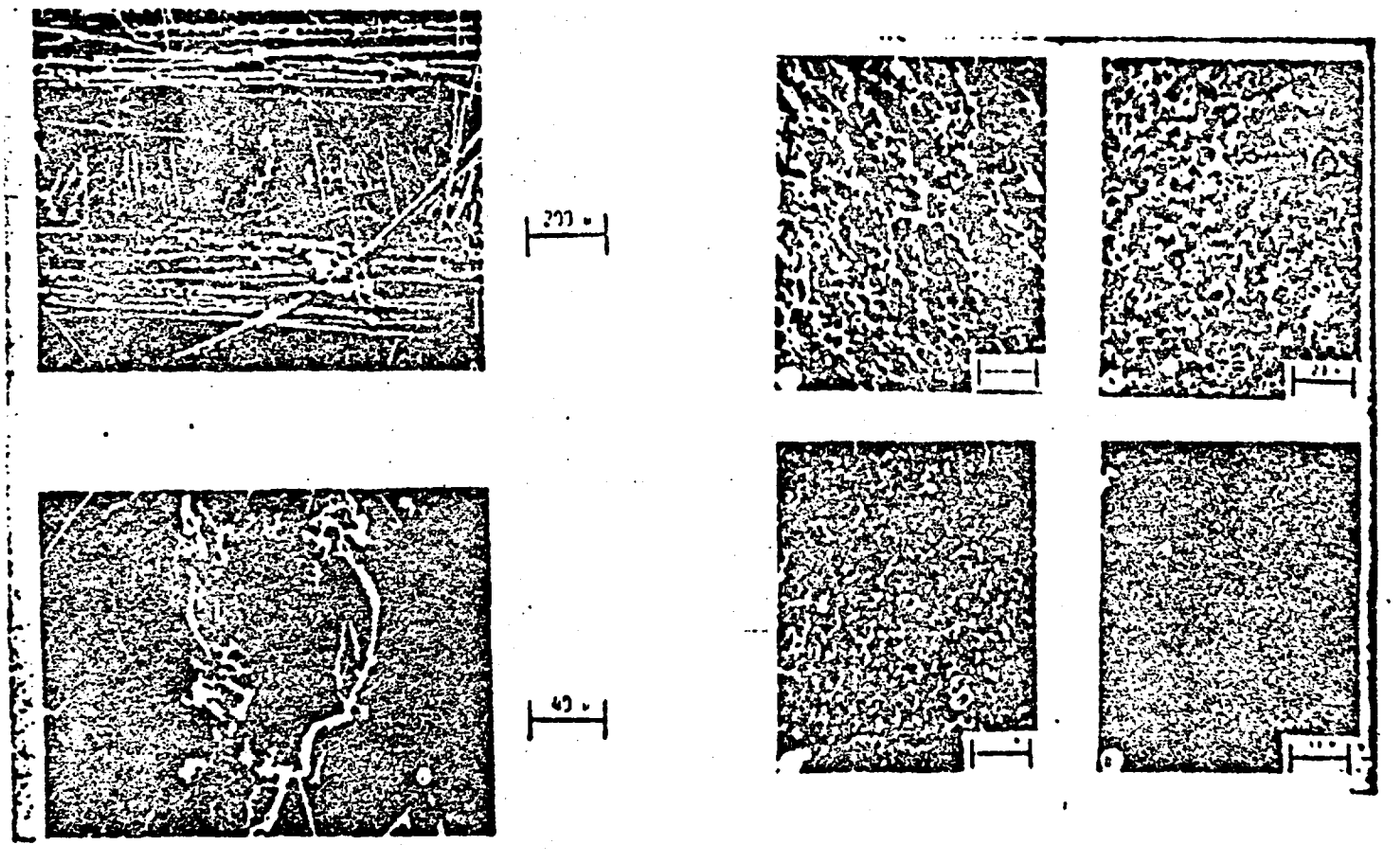

5

6

7

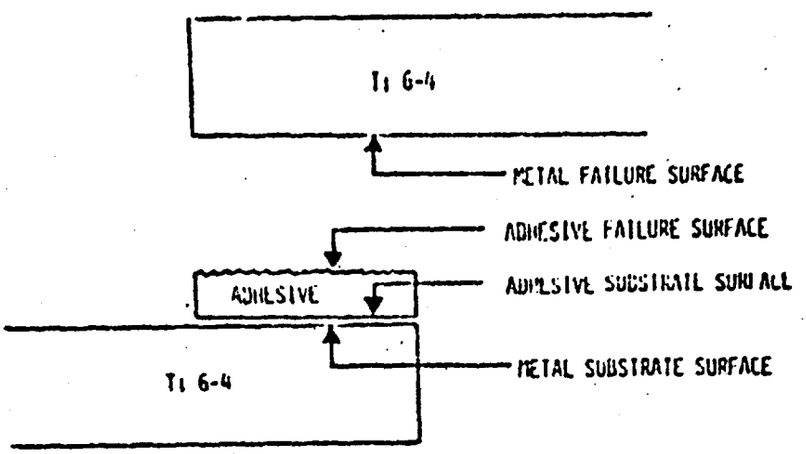
Ti 6-4
METAL FAILURE SURFACE
ADHESIVE FAILURE SURFACE
ADHESIVE
ADHESIVE SUBSTRATE SURFACE
Ti 6-4
METAL SUBSTRATE SURFACE

8

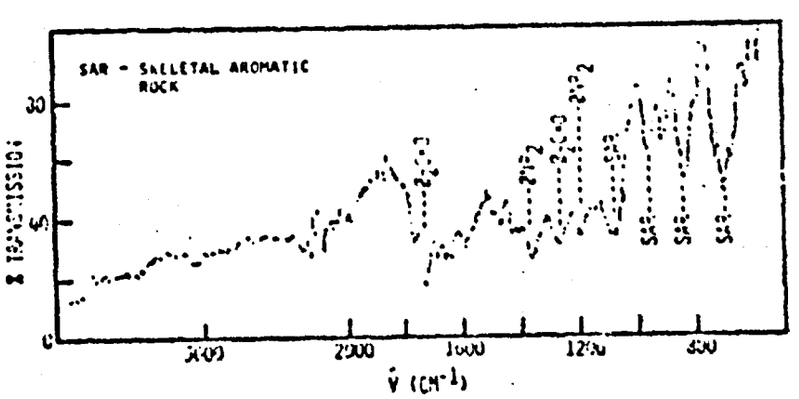
SAR = SKELETAL AROMATIC RING
30
0
2000
1000
ν̄ (CM⁻¹)